

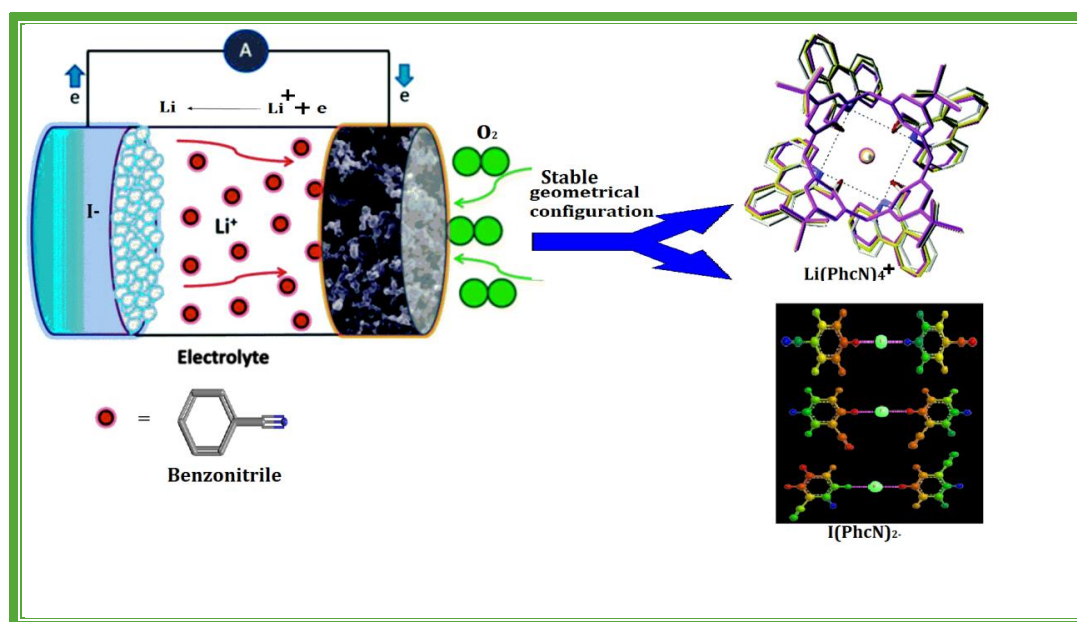
# CHAPTER-VIII

*Studies of Solvation behaviour of LiI prevailing in diverse solvent systems conductometrically and spectrometrically supported by ab-initio technique*

## Highlights ⇒

- Consequences of vibrational spectroscopic data were compared with experimental values.
- The observed blue shift in the spectrum indicates the interaction of anion with PhcN.
- Lithium-ion battery performance shows enhancements in presence of benzonitrile.

## Graphical Abstract ⇒



*\*Published in Chemical Physics Letters 671 (2017) 7-14*

## Abstract

Solvation nature of Lithium iodide (LiI) for both polar and nonpolar organic solvents viz., acetonitrile and benzonitrile have been explored by effect of geometry, spectroscopic, conductometric, ab initio methods. Results of vibrational spectroscopic

data were compared with experimental values. Centre of attraction is iodide anion on significant vibrational bands of benzonitrile. Fluorescence spectra provide a supporting to the mentioned facts. Ab initio calculations used for shaping the optimum location of  $\text{Li}^+$  and  $\text{I}^-$  ions in ion-solvent interactions containing varying nitriles as solvent sphere. Emission band positions, intensity, shape of solvent-sensitive molecules in organic solvents of varying polarities are studied.

## 1. Introduction

The origin of exceptionally elevated solubility of anhydrous lithium iodide in organic solvent system has been a matter of some conjecture. This univalent salt of a small cation and a large anion must possess a favorable balance of lattice and solvation energies conducive to extensive solubility in a broad range of solvents. The solubility and stability of lithium iodide have encouraged its use in studies of salt effects in organic reactions. So it can be said that behaviour in which cations are solvated in solution retains interest for immeasurable applications. Acetonitrile has numerous uses, including as a solvent, for spinning fibers, and in [lithium](#) batteries. Benzonitrile is a useful solvent and a versatile precursor to several derivatives. The benzonitrile ligands are readily displaced by hard centre, making benzonitrile complexes useful synthetic intermediates [1-2].

Vibrational spectroscopy is a consequence of elasticity that explains the truth; atoms in a molecule do not remain in fixed relative positions but vibrate about some mean position. It is a helpful practical tool in order to study ion-solvent interactions in electrolyte solutions. In our current study, FTIR spectroscopic method was used for studying interactions of  $\text{LiI}$  with a variety of aprotic solvents, acetonitrile and benzonitrile. When a spectroscopic records for acetonitrile solution of  $\text{LiI}$  were examined, it was portrayed that both  $\text{Li}^+$  and  $\text{I}^-$  affected the CN stretching frequency; on the other hand, in benzonitrile solution of  $\text{LiI}$ , only the effect of  $\text{Li}^+$  was observed [ 3, 4].

Extensive studies on electrical conductivity investigations have demonstrated the electrolytic properties of solutions of lithium iodide in such diverse materials as acetonitrile and benzonitrile. Renewed interest in the character of electrolyte solutions from the chemical or solvation point of view, it was felt that determination of the solubility trends of lithium iodide would yield some insight into its solution processes

when polar aprotic solvent compared with respect to non-volatile organic solvents in recent years to examine the nature and magnitude of ion-ion and ion-solvent interactions [5, 6]. In the present analysis, the role of the  $\text{Li}^+$  in determining spectral features in acetonitrile could be more carefully assessed by comparison with spectra obtained in the presence of the benzonitrile solvent. Ab initio quantum mechanical calculations were carried out to describe the significant features of the infrared spectrum. Minimal atoms forms ion-solvent cluster in the occurrence of an electrolyte. The initial results of these calculations are also presented in this paper and differentiated with the experimental spectroscopic facts. The electronic emission spectra of organic molecules are generally modified in solvation processes. Fluorescence spectroscopy and imaging have a very broad spectrum of applications for detection and characterization of bimolecular dynamics and interactions in diverse environments.

## **2. Experimental**

### **2.1. Materials**

Lithium iodide (LiI) of puriss grade was procured from Aldrich, Germany with purity assay of salt being  $\geq 98\%$ . Acetonitrile (AcN) procured from Thomas Baker, India and Benzonitrile (PhcN) procured from Merck, Germany was purified using standard methods. The purity of the ( $\text{CH}_3\text{CN}$ ) was 99.5% and (PhCN) was 99%.

### **2.2. Apparatus and procedure**

Infrared spectra were recorded in 8300 FT-IR spectrometer (Shimadzu, Japan) and the particulars about this instrument have been illustrated previously [7-10].

The Conductance measurements were taken in a Systronic-308 conductivity metre (accuracy  $\pm 0.01$ ) using a dip-type immersion conductivity cell, CD-10, having a cell constant of approximately  $(0.1 \pm 0.001) \text{ cm}^{-1}$ . Measurements were made in a water bath maintained within  $T = (298.15 \pm 0.01) \text{ K}$  and the cell was calibrated by the technique proposed by Lind et al. The conductance data were obtained at a frequency of 1 kHz [11, 12].

The Fluorescence measurements were done with QuantaMaster 40 spectrofluorometer . The output range of the machine was nearly 2 analog (+/- 10 volts) [13, 14].

### 3. Results and discussion

**3.1. Infrared Spectra.** FTIR spectra were obtained for pure acetonitrile (AcN), pure benzonitrile and for 0.45(M) LiI solution in AcN and PhcN. The spectrum of pure AcN as well as the special effects of Li<sup>+</sup> ion and I<sup>-</sup> ion are well-known. Our focus of interest here is to observe whether a monatomic anion, namely iodide, has effect on the spectral properties of PhcN as in case of AcN [15-18].

The spectra of two LiI solutions in AcN and PhcN are compared with that of pure AcN and pure PhcN respectively for the 2220-2320 cm<sup>-1</sup> region in Figure 1(a, b) and Figure 2(a, b). The C≡N stretching frequency for pure AcN is observed at 2253 cm<sup>-1</sup> and for pure PhcN ( $\nu_1$ ) at 2228 cm<sup>-1</sup>. In the presence of LiI, one new band appears at 2272 cm<sup>-1</sup> for LiI solution in AcN and for LiI-PhcN solution no such new band is observed to a certain extent a single band appear at 2256 cm<sup>-1</sup>. These bands are ascribed to the Li<sup>+</sup>.....AcN and Li<sup>+</sup>.....PhcN complexes which corresponds to the C≡N stretch. It is also apparent that the band at 2253 cm<sup>-1</sup> for pure AcN is shifted to lower frequency (i.e., slightly red shifted) at 2251 cm<sup>-1</sup> for LiI solution in AcN, which is attributed to the fact that the I<sup>-</sup> anion interacts with the positive end (methyl group) of the AcN molecular dipole; this effect is transmitted through the C-C bond and therefore is feeble in comparison to the cation interaction. On the other hand, from inspection of the spectral data of pure PhcN and LiI-PhcN solution no such red shifted band is observed towards the low frequency side of 2228 cm<sup>-1</sup> Figure 2(a, b). This may be owing to the fact that the phenyl ring in PhcN having high  $\pi$ -electron density does not act as a positive end in a significant way like in the case of methyl group in AcN. As such the I<sup>-</sup> ion containing a large number of core electrons may not be able to experience an attractive interaction with the phenyl ring in PhcN effectively rather there may be a repulsive interaction.

For pure AcN and LiI-AcN solutions, the spectral statistics are shown in Figure 3(a, b) in the region from 2800-3100 cm<sup>-1</sup>. In the spectrum of pure AcN two peaks are observed at 2940 and 3000 cm<sup>-1</sup> analogous to the symmetrical stretch and asymmetrical stretch of the CH<sub>3</sub> group respectively. In the occurrence of LiI two new bands appear at 2922 and 2978 cm<sup>-1</sup>, which are endorsed to the effects of interaction of the I<sup>-</sup> anion by

means of the symmetrical and asymmetrical stretching modes of the CH<sub>3</sub> group respectively. Somewhat red shifted bands at 2938 and 2998 cm<sup>-1</sup> as shown in Figure 3(b) are attributed to interaction of the Li<sup>+</sup> cation at the negative end of the AcN molecular dipole with the CH<sub>3</sub> vibrational modes; this effect is transmitted through both the C≡N and C–C bonds to the CH<sub>3</sub> group and therefore is feeble in comparison to the anion interaction. On the other hand, spectral analysis for pure AcN and LiI–AcN solutions are given in Figure 4(a, b) in same 2800–3100 cm<sup>-1</sup> range. Two bands at 3066 and 3088 cm<sup>-1</sup> are observed for pure PhcN corresponding to the symmetrical (ν<sub>2</sub>) and asymmetrical stretch (ν<sub>3</sub>) of the five C–H bonds in phenyl ring. Two such bands observed for pure PhcN shifts towards lower frequency region in the presence of LiI giving corresponding bands at 3034 (symmetrical stretch) and 3070 cm<sup>-1</sup> (asymmetrical stretch), which are attributed to the effects of interaction of the I<sup>-</sup> anion with the vibrational modes as in the case of LiI–AcN solution. It is also seen from the spectral data of LiI–PhcN solution, no such slightly red shifted bands are observed around the bands at 3066 and 3088 cm<sup>-1</sup>. This may be attributed to the fact that the effect of interaction of Li<sup>+</sup> cation transmitted through both the C≡N and C–C bonds to the C–H groups of the phenyl ring is significantly very weak in comparison to that in LiI–AcN solution.

Spectral data for pure AcN and LiI–AcN solutions in the 890–950 cm<sup>-1</sup> are shown in Figure 5(a, b). Pure AcN shows a band at 918 cm<sup>-1</sup> and LiI–AcN solution shows two bands at 916 and 930 cm<sup>-1</sup>. This band corresponds to C<sub>ipso</sub>–C<sub>nitrile</sub> stretch. New bands at higher frequency 930 cm<sup>-1</sup> and a slightly red shifted band at 916 cm<sup>-1</sup> for LiI–AcN solution are attributed to result of Li<sup>+</sup>·····AcN complex and a little effect of I<sup>-</sup>·····AcN complex, respectively. On the other hand, spectral data in same region from 890–950 cm<sup>-1</sup> for each of pure PhcN (ν<sub>4</sub>) and Li–PhcN solution shows a individual single band at 926 and 939 cm<sup>-1</sup> in Figure 6(a, b) corresponding to C<sub>ipso</sub>–C<sub>nitrile</sub> stretch. The higher frequency band at 939 cm<sup>-1</sup> is ascribed to Li<sup>+</sup>·····PhcN complex. For Li–PhcN solution no such red shifted band is observed as in case of Li–AcN solution, which predicts no interaction of I<sup>-</sup> with the ipso-Carbon of PhcN solvent molecule.

For pure AcN and LiI–AcN solutions, spectral data in the 700–820 cm<sup>-1</sup> range are given in Figure 7(a, b). Pure AcN shows an individual band at 749 cm<sup>-1</sup> and LiI–AcN solution shows two bands at 750 and 765 cm<sup>-1</sup>. These bands correspond to C–C≡N bending mode. New band at higher frequency, 765 cm<sup>-1</sup>, and a slightly blue shifted band

at  $750\text{ cm}^{-1}$  for LiI–AcN solution are recognized to effect of  $\text{Li}^+\cdots\text{AcN}$  complex and a small effect of  $\text{I}^-\cdots\text{AcN}$  complex, respectively. On the other hand, spectral data in the same region from  $700\text{--}820\text{ cm}^{-1}$  for each of pure PhcN ( $\nu_5$ ) and Li–PhcN solution shows a single band at  $758$  and  $774\text{ cm}^{-1}$  shown in Figure 8(a, b) respectively corresponding to the C–C $\equiv$ N bending modes. The higher frequency band at  $774\text{ cm}^{-1}$  is attributed to  $\text{Li}^+\cdots\text{PhcN}$  complexation. As in case of LiI–AcN solution, a blue shifted band is not observed for Li–PhcN solution leads to the prediction that there is no involvement of the formation of  $\text{I}^-\cdots\text{PhcN}$  complex [19-22].

### 3.2. Ab Initio Quantum Chemical Calculations.

In this work, numerical calculations have been performed using UB3LYP functional. Diffused basis functions have often been found to be effective in describing weak interaction among atoms. Hence we use 6-31+G(d) basis function for a correct description of weak interactions which may prevail in the transition structures. These calculations are implemented through Gaussian 09W quantum chemical package.

The quantum chemical calculations estimates that the  $\text{Li}^+\cdots\text{AcN}$  and  $\text{I}^-\cdots\text{AcN}$  complexes would predominantly exists as  $\text{Li}(\text{AcN})_4^+$  [Scheme 1] and  $\text{I}(\text{AcN})_2^-$  [Scheme 2] clusters in the solvent sphere. Similarly we focus on the existence of  $\text{Li}^+\cdots\text{PhcN}$  and  $\text{I}^-\cdots\text{PhcN}$  complexes as clusters through quantum chemical calculations and we hereby compare calculated spectral values with the experimental spectral values in order to explain the shifts [23, 24].

Several of the estimated properties of  $\text{Li}(\text{PhcN})_n$  clusters for cases  $n=1\text{--}4$  are summarized in Table 1. The stabilization of  $\text{Li}(\text{PhcN})_n$  clusters is revealed by the value of  $E$ , the optimization energy, which decreases in magnitude with the number of PhcN molecules up to four. From the calculation,

$\text{Li}(\text{PhcN})_4^+$  was found to be additional stable than other complexes as it has minimum value of  $E$ . For the clusters with  $n>4$  the value of  $E$  once more increases. The optimum solvation number used for  $\text{Li}^+$  in PhcN is, accordingly four. Specifically, the optimum geometry would involve a central  $\text{Li}^+$  ion tetrahedrally surrounded by four benzonitrile molecules [Scheme 1].  $\text{Li}^+\text{--N}$  distance in the complex increases from  $1.88\text{ \AA}$  in  $\text{Li}(\text{PhcN})^+$  to  $2.89\text{ \AA}$  in  $\text{Li}(\text{PhcN})_4^+$ . From Table 1 it is clear that when PhcN solvent fragment act as a

ligand, the  $C\equiv N$  and  $C_{\text{ipso}}-C_{\text{nitrile}}$  bond lengths decreases respectively by 0.01–0.02 Å and 0.003 Å in the  $\text{Li}(\text{PhcN})_n$  cluster with  $n=1-4$  like in the case of  $\text{Li}(\text{AcN})_n$  cluster [25, 26]. Calculated frequencies for  $C\equiv N$  ( $\nu_1$ ),  $C_{\text{ipso}}-C_{\text{nitrile}}$  ( $\nu_2$ ) stretching modes and  $C-C\equiv N$  ( $\nu_3$ ) bending modes in pure PhcN and  $\text{Li}^+\cdots\text{PhcN}$  complexes are compared by way of the experimental results in Table 2. The  $\nu_1$ ,  $\nu_2$  and  $\nu_3$  bands are all shifted in blue direction in agreement with experimental results in Table 2. The blue shift is attributed to charge transfer from a lone pair on the N-atom of PhcN to the  $\text{Li}^+$  ion which promote results to increase in  $C\equiv N$  bond strength and also increases its frequency. This effect is transmitted throughout the molecule and as such blue shifts are moreover observed for  $\nu_2$  and  $\nu_3$  bands. Such frequency shift values are observed to decrease with increase in the number of PhcN ligands in the region of  $\text{Li}^+$  ion. These shifts as summarized in Table 2 are too great in comparison with experiment. Estimation of these quantities could be made better by carrying out quantum chemical calculations with a more enhanced basis sets.

Estimated properties of  $\text{I}(\text{PhcN})_n$  clusters for  $n=1-2$  are given in Table 3. From the quantum chemical calculations,  $\text{I}(\text{PhcN})_2^-$  was found to be more stable as it has least  $E$  value than  $\text{I}(\text{PhcN})^-$ . For the clusters with  $n>2$  value of  $E$  again increases. That is, the optimum geometry would predominantly involve a central I<sup>-</sup> ion linearly surrounded by two benzonitrile molecules in such a fashion that I<sup>-</sup> interacts with H atom resulting in the minimum repulsion between two benzonitrile molecules than other geometry [Scheme 2]. The I<sup>-</sup>-H distance in  $\text{I}(\text{PhcN})^-$  is about 0.03 Å longer than in  $\text{I}(\text{PhcN})^-$  complex. The C-H bond distances slightly decreases by 0.005 Å and the C-C and  $C\equiv N$  distances almost remains equivalent from  $\text{I}(\text{PhcN})^-$  to  $\text{I}(\text{PhcN})_2^-$ . Finally it should be noted that calculations were limited up to  $n=1-2$  PhcN molecules since the number of electrons in the system becomes very large with more solvent molecules [27].

In support of  $C\equiv N$  ( $\nu_1$ ) and  $C_{\text{ipso}}-C_{\text{nitrile}}$  ( $\nu_4$ ) stretching modes and the symmetrical ( $\nu_2$ ) and asymmetrical ( $\nu_3$ ) stretching modes of five C-H bonds in phenyl group of pure PhcN and  $\text{I}^-\cdots\text{PhcN}$  complexes, the calculated frequencies are summarized in Table 4. The red shifted bands  $\nu_1$  and  $\nu_4$  are in agreement with experimental study. On the other hand, the stretching modes ( $\nu_2$  and  $\nu_3$ ) are shifted in blue direction, while the experimentally observed bands are red shifted. This is due to the fact that the C-H bonds in phenyl ring turn out to be significantly stronger. The calculated blue shifted results can be attributed to charge transfer from a lone pair on the I<sup>-</sup> ion to the H atom

resulting in an increase in the C–H bond strength with an enhanced frequency. There would be no change in  $C_{\text{ipso}}-C_{\text{nitrile}}$  and  $C\equiv N$  bond strength which is evidently revealed by the calculated and experimental values [28].

Estimation of the frequencies of IR bands for PhcN from quantum chemical calculation are compared with the experimental data. Theory properly explains the direction of the shifts due to the interaction of PhcN with the ions for  $\nu_1$ ,  $\nu_4$  and  $\nu_5$  bands. Estimated frequency shift values are, however, too large in comparison with experiment. Better quantitative agreement between theory and experiment may result by carrying out quantum chemical calculations with a more superior basis sets. In case of stretching frequencies of five C–H bonds of phenyl group, the estimated shift caused by  $I^-$  is in the opposite direction to the red shift observed experimentally. This may be attributed to the piece of information that the predicted results are based on PhcN dimer. In fact, a more realistic complex may behave differently from theoretical results. The differences between the theoretical and experimental shifts for these bands due to  $Li^+$  are considered to be insignificant [29].

### **3.3. Challenges of ionic conductivity and Conductance studies**

---

The conductance of an electrolyte solution increases with rise in temperature due to the enhancement in extent of ionization. The strong electrolyte LiI, undergo complete ionization and hence illustrate higher conductivities since they furnish more number of ions. As the concentration of the solution increases the molar conductivity decreases as a result of the ion association between  $Li^+$  and PhcN molecules as well as  $I^-$  with PhcN molecules [Figure 9(a), (b), (c)]. But since the temperatures increases the molar conductivity as well as limiting molar conductivity increases, due to weakening of ion pair association Table (5, 6). LiI taken in the polar and non-polar nitriles, which itself is a strong electrolyte retains its identity in both solvents. But due to the higher number of canonical structures in acetonitrile the ion – pair formation which was done in our previous works [30, 31] was unstable. While in the case of benzonitrile, much extra stability is attained in the ion-pair formation as PhcN is a weak electron donor. The limiting equivalent conductance of LiI leads to the conclusion that with the increase in temperature the ionic size becomes much more effective to be entirely associated in the ion-pair formation [32, 33]. Two opposing factors control the state of affairs in solution of electrolytes: (1) the coulombic interaction which tends to arrange the ions in an

ordered and organised structure and (2) the thermal collision between the ions and solvent molecules which tends to prevent the existence of an organised structure in solution. At higher temperature, the structure is still less organised because of increased thermal collision. As a result of the above two opposing factors, a situation arises when the negative ion end up as the nearest neighbours of a given central positive ion and vice versa. Thus, a cation is surrounded by more cations than anions. This gives rise to the ionic atmosphere where the central ion is surrounded by a group of ions of opposite charges. Thus as the temperature increases the electrophoretic effect as well as asymmetry effect decreases making ion pair formation predominant over ion-solvent one [34-36].

### **3.4. Fluorescence study**

The improvement of fluorescent Lithium ion sensors is a vigorous research area. Lithium ion sensors are currently in demand for biomedical applications and for monitoring ion transport in lithium ion batteries.  $\text{Li}^+$  sensors have been reported in the present study, in the presence of acetonitrile and benzonitrile in the solution phase. In the first case of  $\text{Li}^+$  ion – acetonitrile there was no notable change. The present work involves a similar investigation of the benzonitrile-Lithium iodide systems. Next on proceeding towards pure PhcN. Benzonitrile is of particular interest because of its large dipole moment and of the presence of two active sites of molecular interaction i.e. the benzene ring and the C---N  $\pi$  electron containing substituent. A fluorescence study of benzonitrile had been reported previously in [37, 38] depicted that excitation of  $95\text{cm}^{-1}$  showed the most intense dimersed form of PhcN and even at  $113\text{cm}^{-1}$  and  $49\text{cm}^{-1}$  distinct bare bands had been predicted. Upon adding of LiI a new spectrum arises. The stock of LiI and benzonitrile was prepared in the range of  $10^{-3}(\text{M})$  concentration and the various fragments were made from it. It was noticed that on increasing the concentration of the ions complexation leading towards ion-solvent interaction also increases that means more benzonitrile molecules are engaged to form complex either with  $\text{Li}^+$  ion or with  $\text{I}^-$  ion ; which will reduce the fluorescence intensity of benzonitrile to some lower energy region. Indeed it was proven previously  $\text{I}^-$  interaction has more significance than  $\text{Li}^+$ . LiI–benzonitrile system excitation was set at 113 nm and emission was observed at 420 nm, as shown in Figure 10. Though from the above mentioned FTIR

spectral data of pure PhcN and LiI-PhcN solution no red shifted band is observed towards the low frequency; the same termination is followed as supporting information of the above mentioned facts through the steady state emission spectrum of the studied metal ion in benzonitrile solvent system. This system thus reveals the fact that a characterized blue shifted spectra would be visible, which explains the fact that upon ionic bonding contradicts the solute – solvent interaction to be most probably ion-dipole interaction or the ion-solvent interaction based upon ab initio quantum mechanical calculations. It is interesting to note that the solubility, stability in structure of LiI-benzonitrile is more than that in acetonitrile. Thus it is an important proof towards the ion-solvation of PhcN with I<sup>-</sup>.

#### **4. Novelty of the studied dissertation**

Aromatic nitriles have extensive applications in the manufacture of dyes, pesticides and pharmaceuticals. They are used as intermediates in synthesis of a variety of pharmacologically active compounds which are used as sedatives, muscle relaxants, neuroleptics, etc. Benzonitriles are of vast interest in the ground of organic chemistry for the synthesis of pharmaceuticals, natural products, herbicides, and agrochemicals. In the current work substituted benzonitriles are being studied in order to find its novelty in many reactions in industries at high temperatures. Moreover benzonitrile acquire high stability; it is more resistant to breaking down or decomposition. The thermal stability is also measured in the processing, long-term storage. The higher stability as well helps to avoid runaway reactions. Thus, it is vital to search for an alternate strategy that can improve the stability of chemical compounds by altering their physical, thermal or structural and bonding properties. Lithium-ion battery performance is strongly influenced by the ionic conductivity of the electrolyte, which depends on the speed at which Li ions drift across the cell and relates to their solvation structure. The choice of solvent can greatly impact both solvation and diffusivity of Li<sup>+</sup> ions. Schematically the action of these batteries occurs together with an exchange of ions between the solution and the electrodes. The FTIR spectroscopic analysis of benzonitrile and acetonitrile was carried out to evaluate the impact of at atomic and molecular level like bond strength, stability, rigidity of structure, etc. As latest supplies and strategies are found, Li-ion batteries will no doubt have an ever superior impact on our lives in the years to come [39-49].

## 5. Conclusion

The effect of cations on the infrared spectrum of AcN is well known. Similarly, we have focused on the effect of anion on infrared spectrum of PhcN. Here the effect of anion on the spectral properties of PhcN based on quantum chemical calculations is in agreement with the experimental observations. The effect of the anion is clearly seen in the spectra only for five C–H bonds in phenyl group. Interaction of the anion with PhcN occurs at the phenyl hydrogen atoms in such a way that the blue shift is observed for symmetrical and asymmetrical vibrations. The most important prediction is that the anion has no any change on spectral properties of  $C\equiv N$ ,  $C_{\text{ipso}}-C_{\text{nitrile}}$  and  $C-C\equiv N$  bands which confirms that there is no any interaction with ipso-Carbon; this may be attributed to the presence of bulky phenyl group. All these theoretical and experimental observations are especially helpful in understanding the changes in the spectral features that are observed when the electrolyte, LiI, is added to PhcN. Rechargeable Li-based batteries have been broadly investigated due to their excellent energy and power density.

**Keywords:** Acetonitrile, Benzonitrile, Ion-solvation, Lithium Iodide, Vibrational wave numbers.

### Notes and References

1. D.Ekka and M.N. Roy\*, RSC Adv., 4, (2014) 19831.
2. Yuan K, Bian H, Shen Y, Jiang B, Li J, Zhang Y, Chen H, and Zheng J., The Journal of Physical Chemistry B, 118, (2014) 3689-3695.
3. Cho J S, Cho H.G\*, Bull. Korean Chem. Soc., 30, (2009) 803-809.
4. S.O. and [Murphy C J.\\*](#), Inorg. Chem., 40, (2001) 6080-6082.
5. [D. M. Seo](#),<sup>a</sup> [P. D. Boyle](#),<sup>b</sup> [O. Borodin](#)<sup>c</sup> and [W. A. Henderson](#)<sup>\*a</sup>., RSC Adv., 2, (2012) 8014-8019.
6. P. [Hobza](#) and Z. [Havlas](#) , Chem. Rev., 100, (2000) 4253–4264.
7. D. Ekka, M. N.Roy, The Journal of Physical Chemistry B, 116, (2012) 11687-11694.
8. T. Ray and M. N. Roy\*, RSC Adv., 5, (2015) 89431.
9. D.[Ekka](#), T.[Ray](#), [K. Roy](#), and [M.N.Roy](#), J. Chem. Eng. Data, 61, (2016) 2187–2196.

10. M.N.Roy, M.C Roy, S. Choudhury, P.K. Roy, R. Dewan, *Thermochimica Acta*, 599, (2015) 27–34.
11. A.Sinha, A.Bhattacharjee, M. N. Roy, *J. Dispersion Sci. Technol.*, 30, (2009) 1003–1007.
12. M.C.Roy, M. N.Roy, *Journal of Molecular Liquids*, 195, (2014) 87–91.
13. M.N.Roy, M.C.Roy and K. Roy, *RSC Adv.*, 5, (2015) 56717.
14. M. Homocianu, A Airinei, and D.O.Dorohoi, *Journal of Advanced Research in Physics*, 2, (2011) 11105.
15. R. Bhattarai, B. Roy , P.Guha , A. Bista , A. Bhadra , G. Karmakar , P. Nahak , P. Chettri and A. K. Panda, *J. Surface Sci. Technol.*, 31, (2015) 77–85.
16. A. Gladney, C. Qin and H. Tamboue, *Open Journal of Physical Chemistry*, 2, (2012) 117-122.
17. J. R. Reimers and L. E. Hall, *Journal of the American Chemical Society*, 121, (1999) 3730-3744.
18. S. S. Andrews and S. G. Boxer, *The Journal of Physical Chemistry A*, 104, (2000) 11853-11863.
19. K.-I. Oh, J.-H. Choi, J. Lee, J. Han, H. Lee and M. Cho, *The Journal of Chemical Physics*, 128, (2008) 154504-154511.
20. A. K. Mollner, P. A. Brooksby, J. S. Loring, I. Bako, G. Palinkas, and W. R. Fawcett, *J. Phys. Chem. A* 108, (2004) 3344-3349.
21. [S. Zhang](#), [Y. Zhang](#), [X. Ma](#), [L. Lu](#), [Y. He](#), [Y. Deng\\*](#), *J. Phys. Chem. B*, 117, (2013) 2764–2772.
22. D. Bhattacharjee, A. Ghosh (Purkayastha), T. N. Misra, S. K. Nandy. *Journal of Raman Spectroscopy*, 27, (1996) 457–461.
23. Y. Koga, S. Kondo, S. Saeki, and W. B. Person, *The Journal of Physical Chemistry*, 88, (1984) 3152-3157.
24. [Bakó, Imre](#); [Megyes, Tünde](#); [Pálinkás, Gábor](#), *Chemical Physics*, 316, (2005) 235-244.
25. [D. Spångberg](#), [Kersti Hermansson](#), *Chemical Physics* , 300(1), (2004) 165-176 .
26. [R. Rivelino](#), [B.J.C .Cabral](#), [K. Coutinho](#), [S. Canuto](#), *Chemical Physics Letters*, 407, (2005) 13-17.
27. T. A. Ford, L. Glasser, *Int. J. Quantum Chem.*, 84, (2000) 226–240.
28. [I. Bakó](#), [T. Megyes](#), [G. Pálinkás](#), *Chemical Physics*., 316, (2005) 235-244.

29. W. Kunz, J. Barthel, L. Klein, T. Cartailier, P. Turq, B. Reindl, *Journal of Solution Chemistry*, 20, (1991) 875–891.
30. M. N. Roy, R. Dewan, D. Ekka, I. Banik, *Thermochimica Acta*, 559, (2013) 46– 51.
31. M. N. Roy, D. Ekka, I. Banik, A. Majumdar, *Thermochimica Acta.*, 547, (2012) 89– 98.
32. R. Dewan, B. Datta, M. C. Roy, M. N. Roy, *Fluid Phase Equilibria.*, 358, (2013) 233–240.
33. F. Lahmani, C. Lardeux-Dedonder, D. Solgadi, A. Zehnaeker, *Chem. Phys.*, 120, (1988) 215.
34. M.A. Rub, A.M. Asiri, A.Z. Naqvi, M.M. Rahman, S.B. Khan, K.U. Din, *J. Molecular Liquids*, 177, (2013) 19-25.
35. M. Rahman, M.A. Khan, M.A. Rub, Md. A. Hoque, *J. Molecular Liquids*, 223, (2016) 716-724.
36. D. Kumar, M. A. Rub, *J. Phys. Org. Chem.*, 29, (2016) 394-405.
37. T. Kobayashi, K. Honma, O. Kajimoto and J. Tshuchiya, *J. Chem. Phys.*, 6, (1987) 1111-1118.
38. F. Lahmani, C. Lardeux-Dedonder, and A. Zehnaeker, *Laser Chem.* 10, (1989) 41-50
39. M.N.Roy, D. Ekka, R. Dewan, *Fluid Phase Equilibria.*, 314, (2012) 113– 120
40. M. N. Roy,\* R. Dewan, and L. Sarkar, *J. Chem. Eng. Data.*, 55, (2010) 1347–1353.
41. S. Saha, A. Roy, K. Roy & M. N. Roy, *Nature Scientific reports*, 6, (2016) 35764.
42. H.Y.Song\*, T. Fukutsuka, K. Miyazaki, T.Abe, *J Appl Electrochem*, 46, (2016) 1099–1107.
43. W. Huang, L.Xing, Y.Wang, M.Xu, W.Li, F.Xie, S.Xia, *Journal of Power Sources*, 267, (2014) 560-565.
44. W.V.Schalkwijk, B.Scrosati, *Advances in Lithium – Ion Batteries*, e-book Springer.
45. R.Rohan, T-C Kuo, J-H Lin, Y-C Hsu, C-C Li and J-T Lee, *The Journal of Physical Chemistry C*, 120, (2016) 6450-6458.
46. Y.Wu, 2015, *Lithium –Ion Batteries: Fundamentals and Applications*, e-book Science.
47. R.T.Jow, K.Xu, O.Borodin, M.Ue, *Electrolytes for Lithium and Lithium – Ion Batteries*, Springer.
48. D.Bandyopadhyay, *Eur.Phys. J. D.*, 54, (2009) 643-655.
49. Q. Li, J.Chen, Y. Lu, *Science Direct: Green Energy & Enviroment*, 1, (2016) 18-42.

TABLES

**Table 1: Properties of Li<sup>+</sup>⋯PhcN Complexes calculated by the UB3LYP/6-31+g(d) method**

Bond length in Å				
Complex	E in a.u	Li–N	C≡N	C–C
PhcN			1.26	1.42
Li(PhcN) <sup>+</sup>	-7286	1.88	1.24	1.42
Li(PhcN) <sub>2</sub> <sup>+</sup>	-7213	1.92	1.24	1.42
Li(PhcN) <sub>3</sub> <sup>+</sup>	-7154	2.17	1.24	1.42
Li(PhcN) <sub>4</sub> <sup>+</sup>	-7022	2.89	1.23	1.42

**Table 2: Estimated vibrational frequencies for Li<sup>+</sup>⋯PhcN complexes**

Frequency of band in cm <sup>-1</sup>				
Complex	v <sub>1</sub>	v <sub>4</sub>	v <sub>5</sub>	
PhcN	2037	901	402	
Li(PhcN) <sup>+</sup>	2143	933	443	
Li(PhcN) <sub>2</sub> <sup>+</sup>	2123	924	448	
Li(PhcN) <sub>3</sub> <sup>+</sup>	2132	918	451	
Li(PhcN) <sub>4</sub> <sup>+</sup>	2111	915	454	

**Table 3: Properties of I<sup>-</sup>⋯PhcN Complexes calculated by the UB3LYP/midix method**

Bond Length in Å					
Complex	E in a.u	I–H	C–H	C <sub>ipso</sub> – C <sub>nitrile</sub>	C–N
I(PhcN) <sup>-</sup>	-980	3.14	1.16	1.47	1.26
I(PhcN) <sub>2</sub> <sup>-</sup>	-1305	3.17	1.16	1.47	1.26

**Table 4. Estimated vibrational frequencies for I<sup>-</sup>⋯PhcN Complexes**

Frequency of Band in cm <sup>-1</sup>				
Complex	v <sub>1</sub>	v <sub>4</sub>	v <sub>2</sub>	v <sub>3</sub>
PhcN	2039	899	3175	3244
I(PhcN) <sup>-</sup>	2028	899	3193	3269
I(PhcN) <sub>2</sub> <sup>-</sup>	2032	899	3189	3265

**Table 5. Molar conductance (Λ) and molar concentration of lithium iodide salts in benzonitrile solution at various temperatures**

C (mol dm <sup>-3</sup> )	T(K)	Λ (Scm <sup>2</sup> mol <sup>-1</sup> )
---------------------------	------	---

<b>0.05</b>	293.15	6.92
<b>0.15</b>	293.15	5.92
<b>0.25</b>	293.15	5.42
<b>0.35</b>	293.15	5.01
<b>0.45</b>	293.15	4.69
<b>0.05</b>	303.15	7.54
<b>0.15</b>	303.15	6.87
<b>0.25</b>	303.15	6.36
<b>0.35</b>	303.15	6.13
<b>0.45</b>	303.15	5.36
<b>0.05</b>	313.15	8.78
<b>0.15</b>	313.15	7.23
<b>0.25</b>	313.15	6.36
<b>0.35</b>	313.15	5.33
<b>0.45</b>	313.15	4.32

**Table 6. Equivalent conductance at infinite dilution at various temperatures of Lithium iodide in benzonitrile solution**

<b>T(K)</b>	<b><math>\Lambda</math> (Scm<sup>2</sup>mol<sup>-1</sup>)</b>
<b>293.15</b>	7.2
<b>303.15</b>	7.98
<b>313.15</b>	9.65

## FIGURES

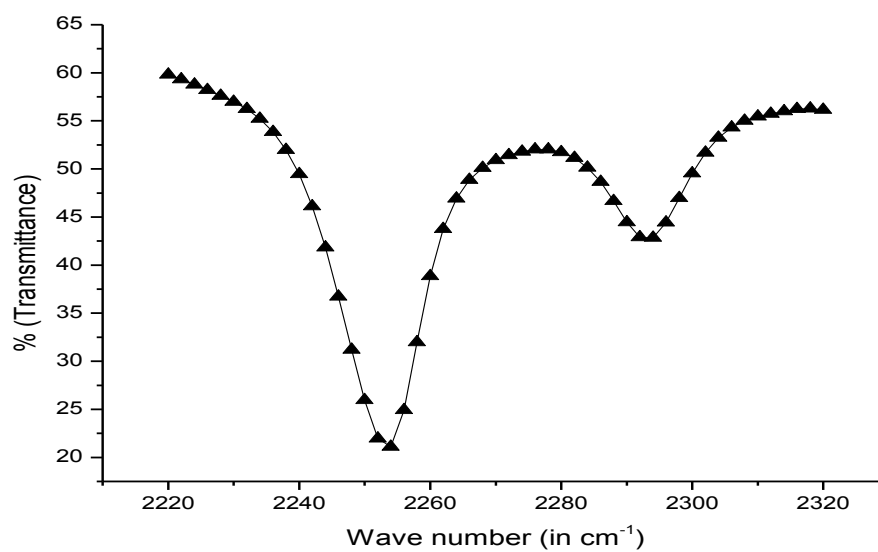


**Figure 1(a).** Infrared spectra for pure AcN in the C≡N stretch region (2220 – 2320 cm<sup>-1</sup>)

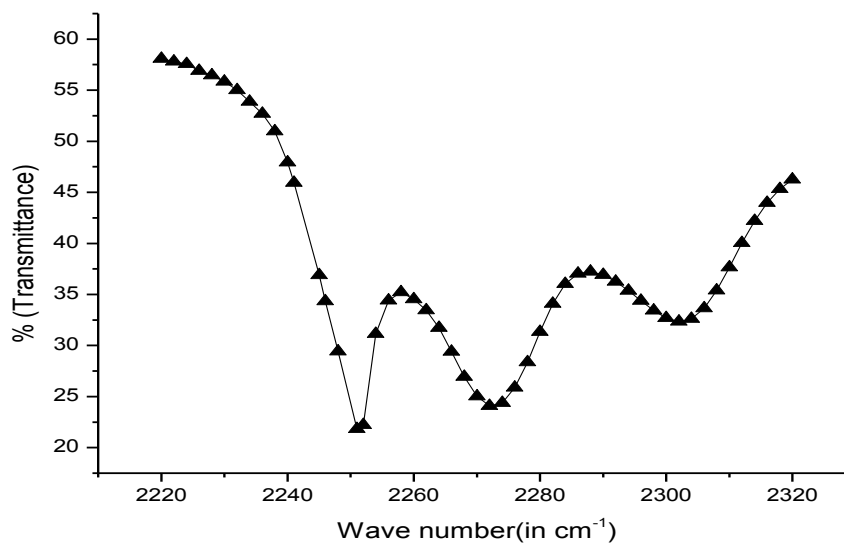


**Figure 1(b).** Infrared spectra LiI-AcN solution in the C≡N stretch region (2220 – 2320 cm<sup>-1</sup>)

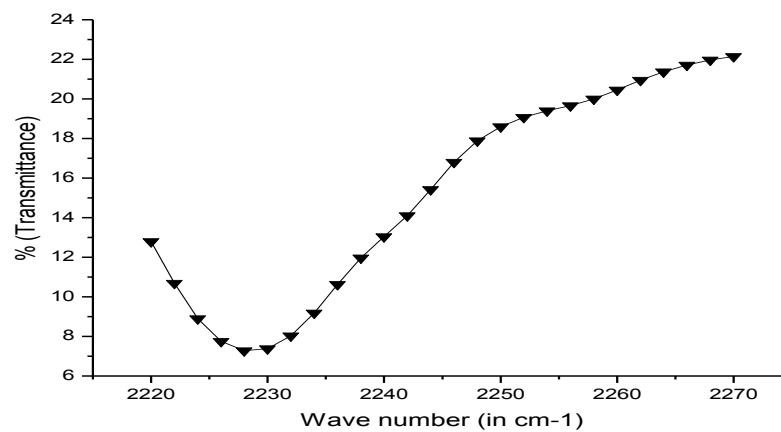


**Figure 2(a).** Infrared spectra for pure PhcN solution in the C≡N stretch region (2220 – 2320 cm<sup>-1</sup>)

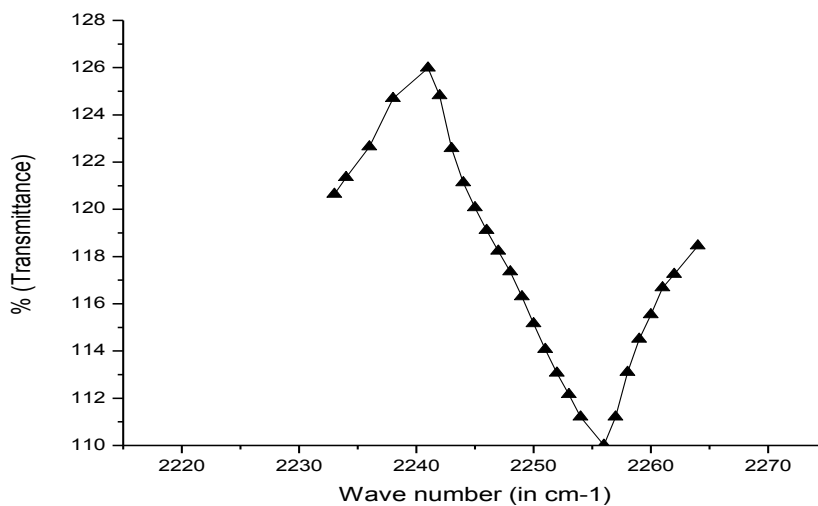


**Figure 2(b).** Infrared spectra for LiI-PhcN solution in the C≡N stretch region (2220 – 2320 cm<sup>-1</sup>)

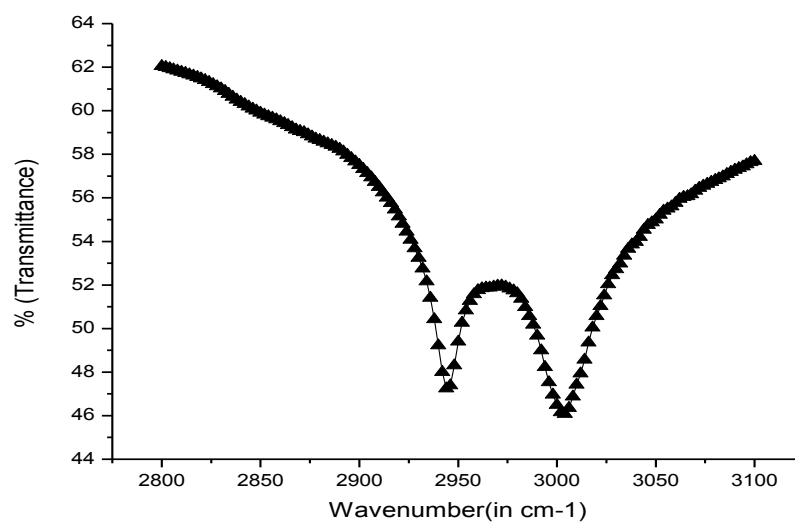


**Figure 3(a).** Infrared spectra for Pure AcN solution in the C–H stretch region (2800 – 3100  $\text{cm}^{-1}$ )

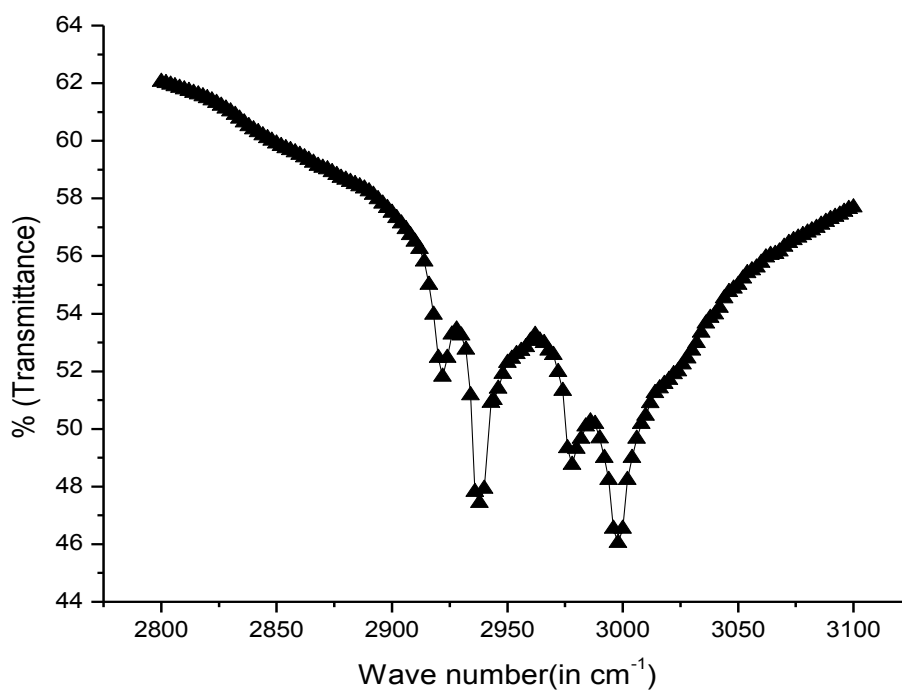


**Figure 3(b).** Infrared spectra for LiI–AcN solution in the C–H stretch region (2800 – 3100  $\text{cm}^{-1}$ )

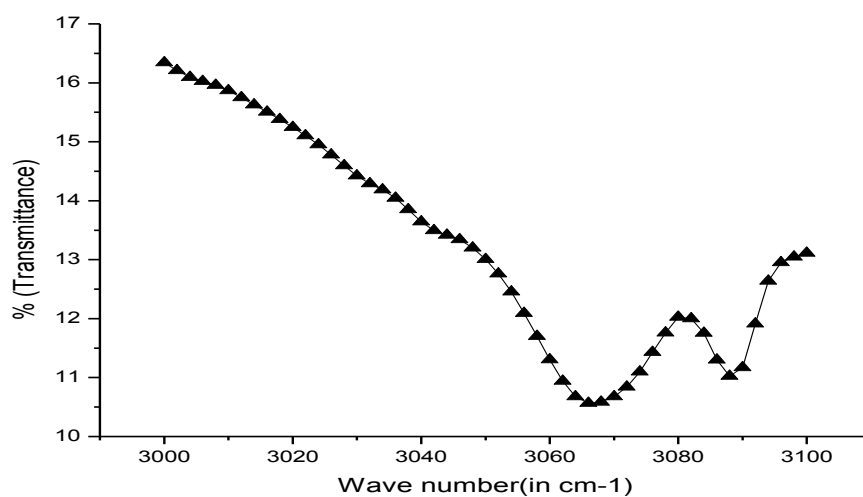


**Figure 4(a).** Infrared spectra for pure PhcN solution in the C—H stretch region (2800 – 3100  $\text{cm}^{-1}$ )

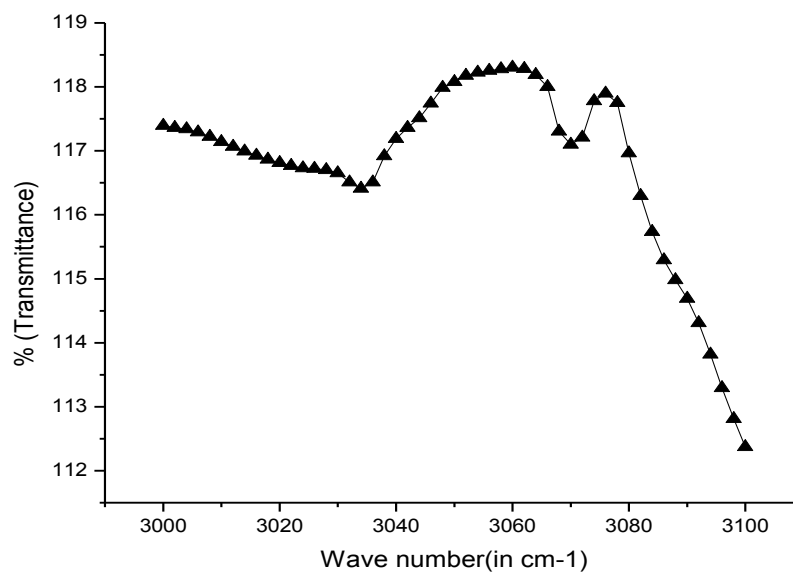


**Figure 4(b).** Infrared spectra for LiI—PhcN solution in the C—H stretch region (2800 – 3100  $\text{cm}^{-1}$ )

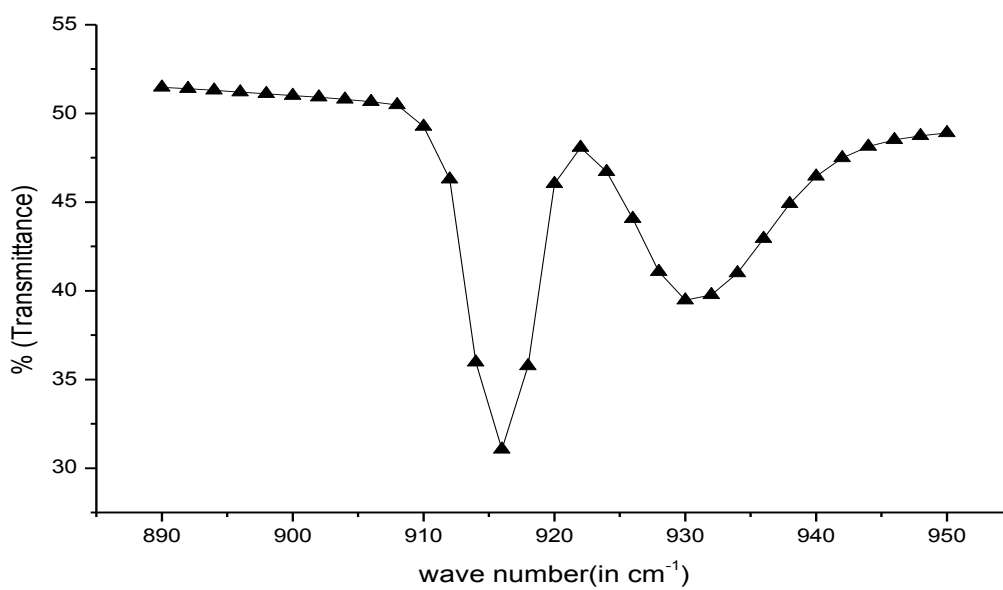


**Figure 5(a).** Infrared spectra for pure AcN solution in the C–C stretch region (890 – 950 cm<sup>-1</sup>)

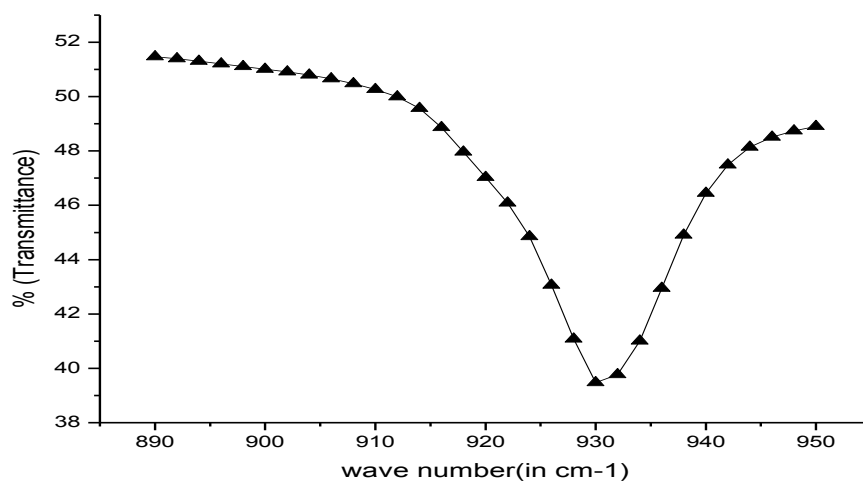


**Figure 5(b).** Infrared spectra for LiI–AcN solution in the C–C stretch region (890 – 950 cm<sup>-1</sup>)

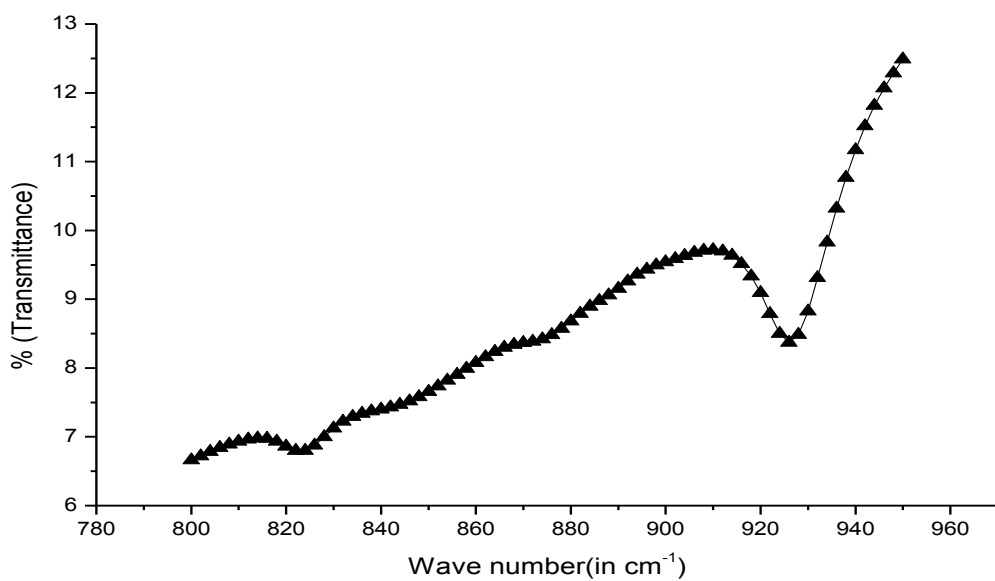


**Figure 6(a).** Infrared spectra for pure PhcN solution in the C—C stretch region (890 – 950  $\text{cm}^{-1}$ )

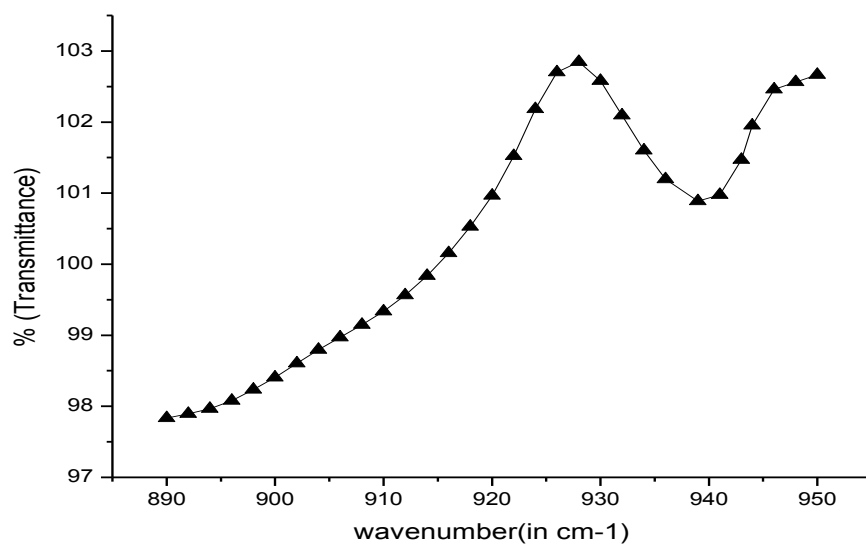


**Figure 6(b).** Infrared spectra for LiI—PhcN solution in the C—C stretch region (890 – 950  $\text{cm}^{-1}$ )

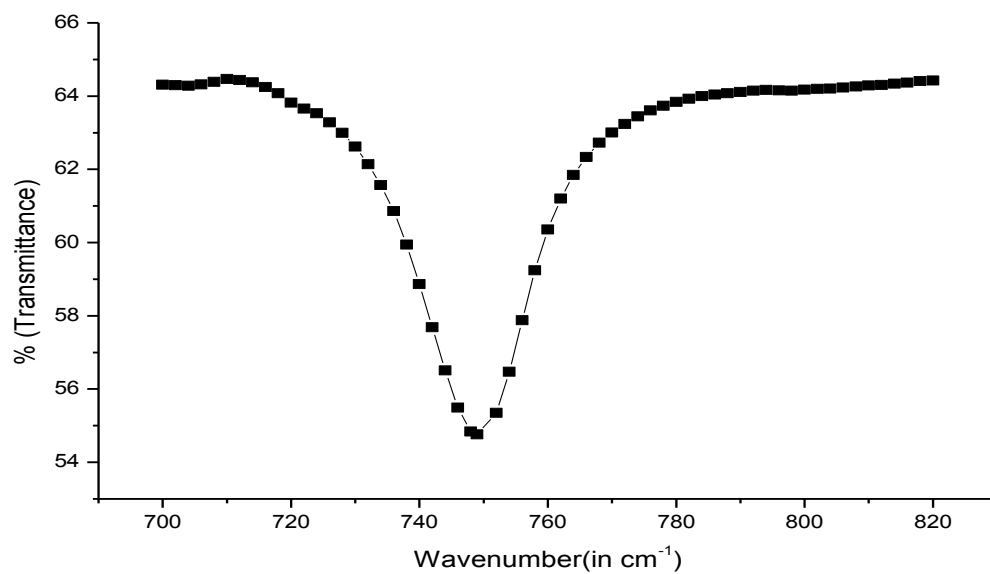


**Figure 7(a).** Infrared spectra for pure AcN solution in the C–C≡N stretch region (700 – 820 cm<sup>-1</sup>)

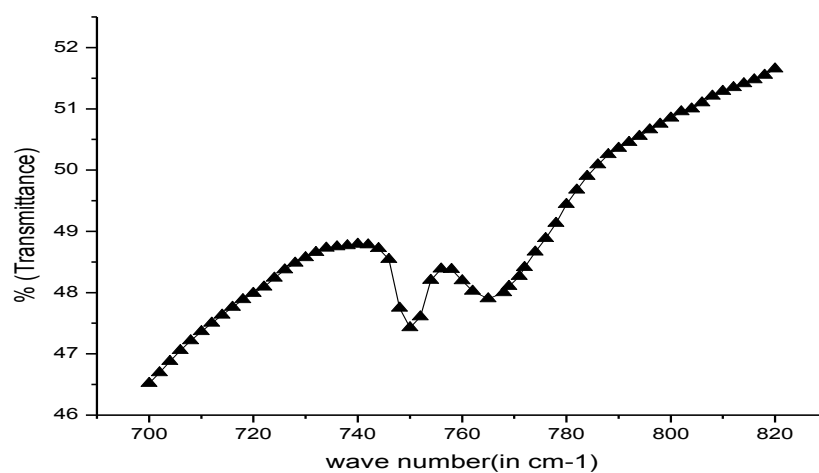


**Figure 7(b).** Infrared spectra for LiI– AcN solution in the C–C≡N stretch region (700 – 820 cm<sup>-1</sup>)

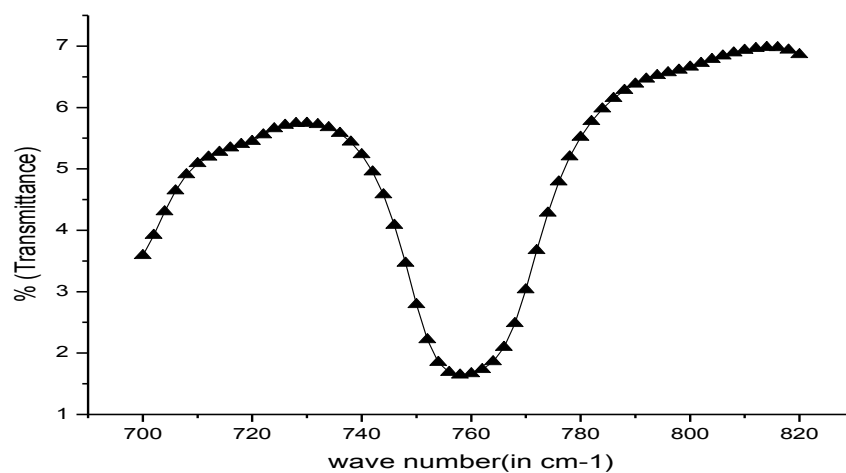


**Figure 8(a).** Infrared spectra for pure PhcN solution in the C–C≡N stretch region (700 – 820 cm<sup>-1</sup>)

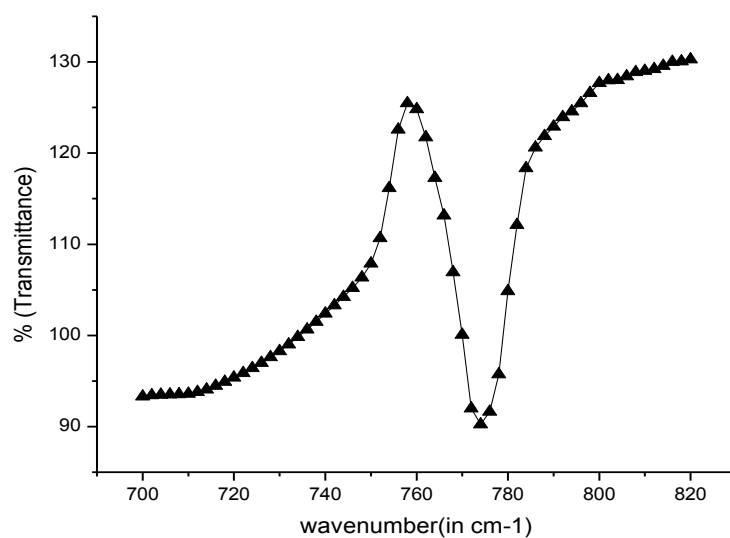


**Figure 8(b).** Infrared spectra for LiI–PhcN solution in the C–C≡N stretch region (700 – 820 cm<sup>-1</sup>)

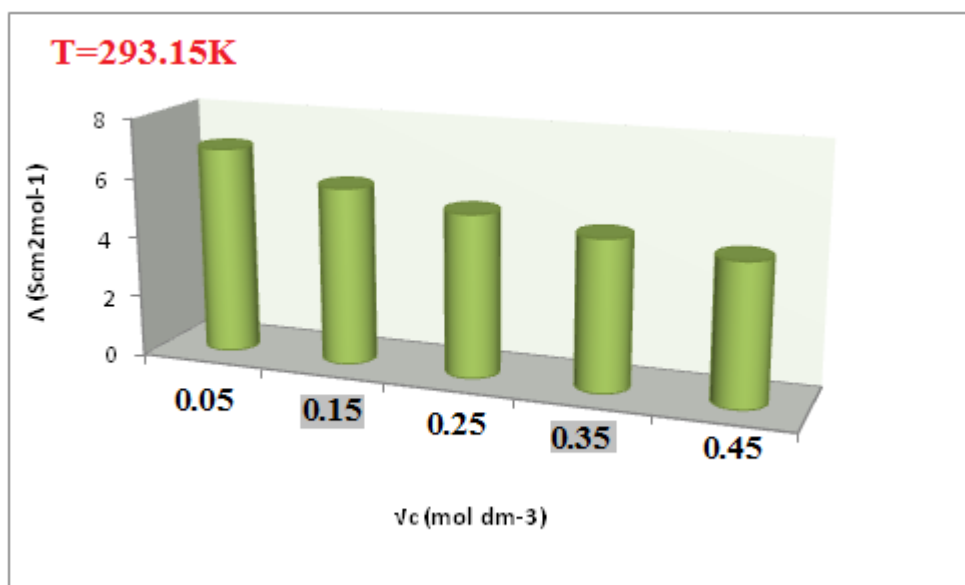


**Figure 9(a).** The plot of  $\Lambda$  vs  $\sqrt{C}$  of lithium iodide in benzonitrile solution at 293.15 K

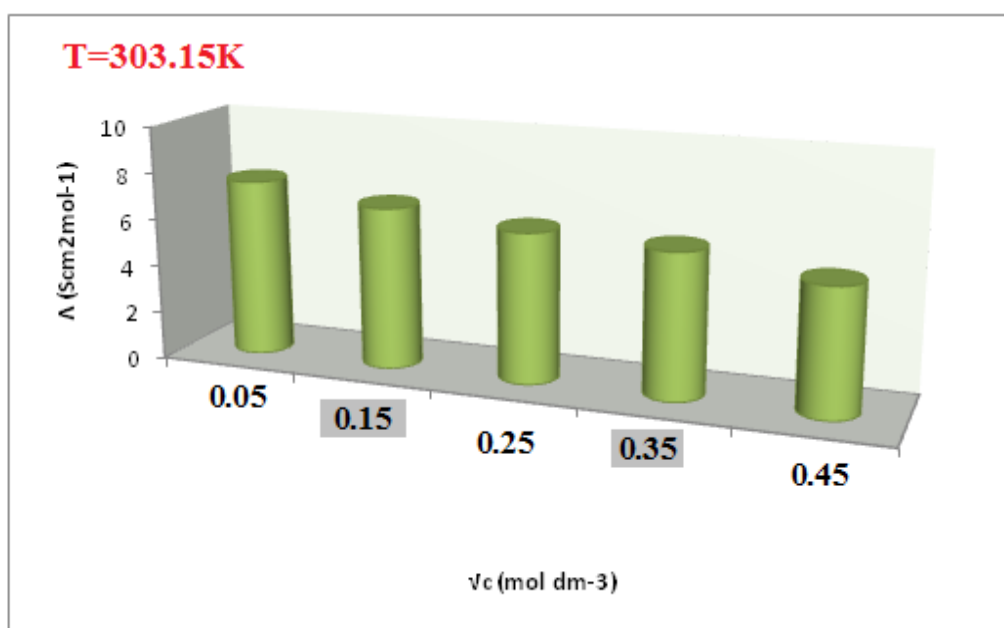


**Figure 9(b).** The plot of  $\Lambda$  vs  $\sqrt{C}$  of lithium iodide in benzonitrile solution at 303.15 K

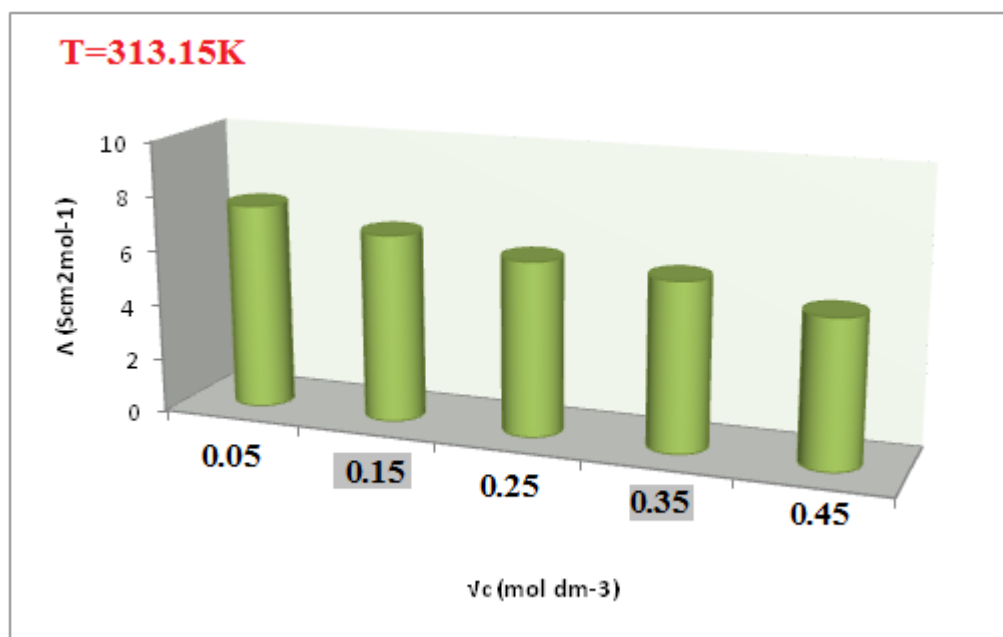


**Figure 9(c).** The plot of  $\Lambda$  vs  $\sqrt{C}$  of lithium iodide in benzonitrile solution at 313.15 K

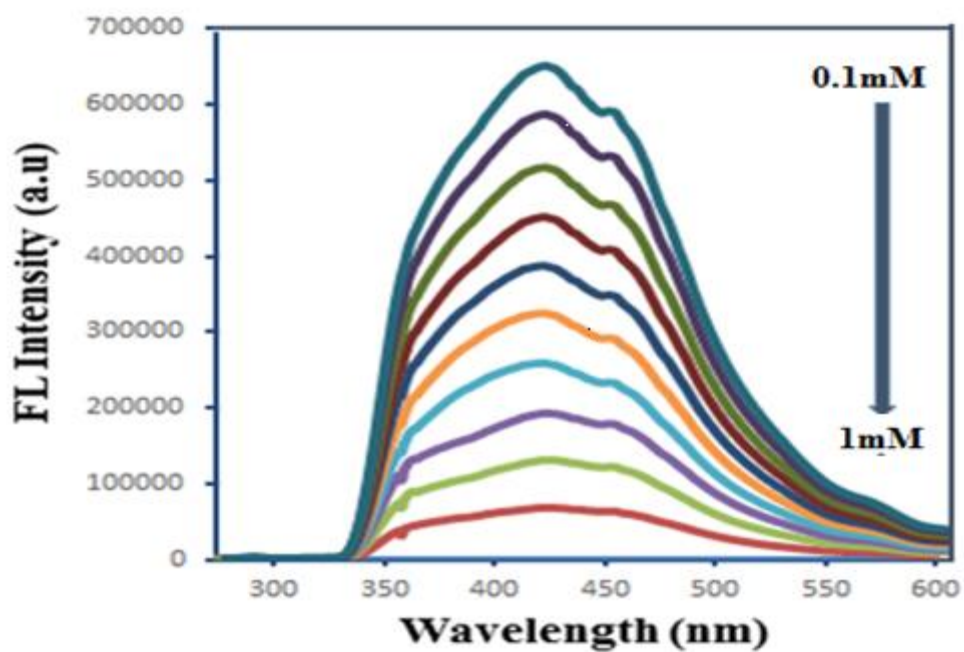
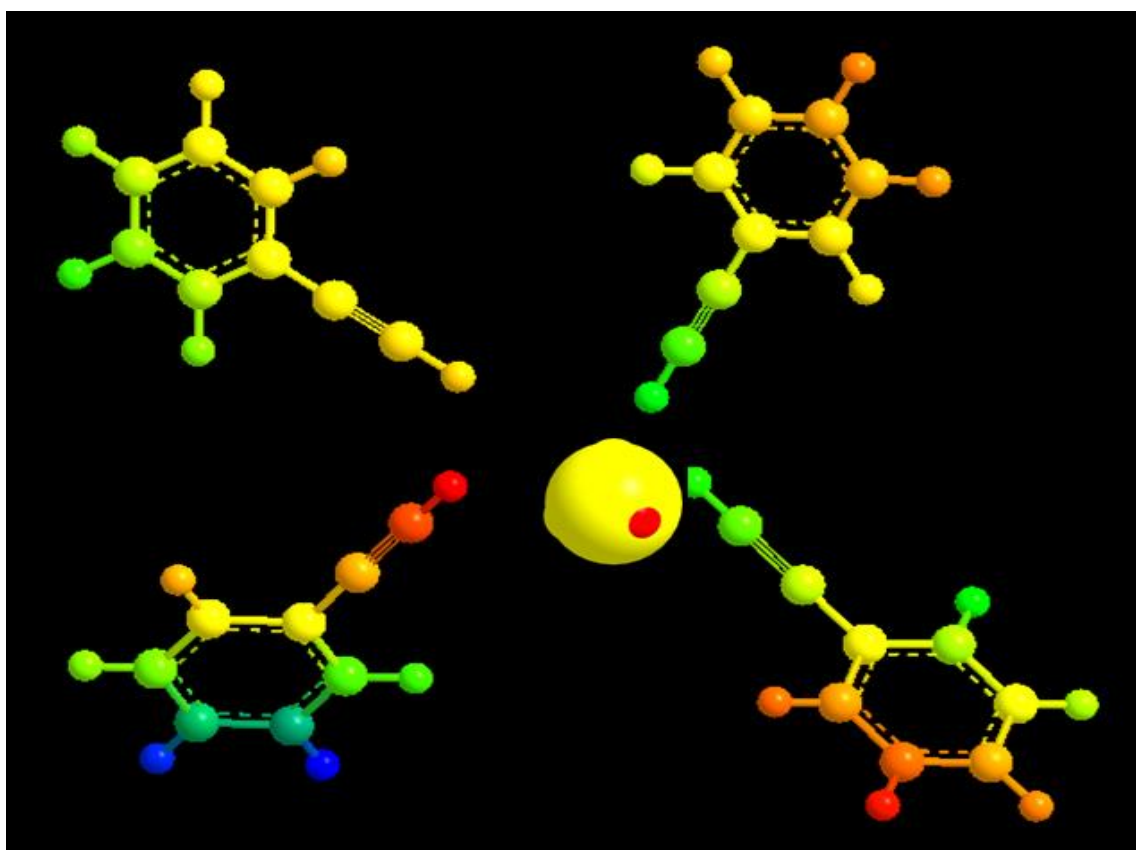


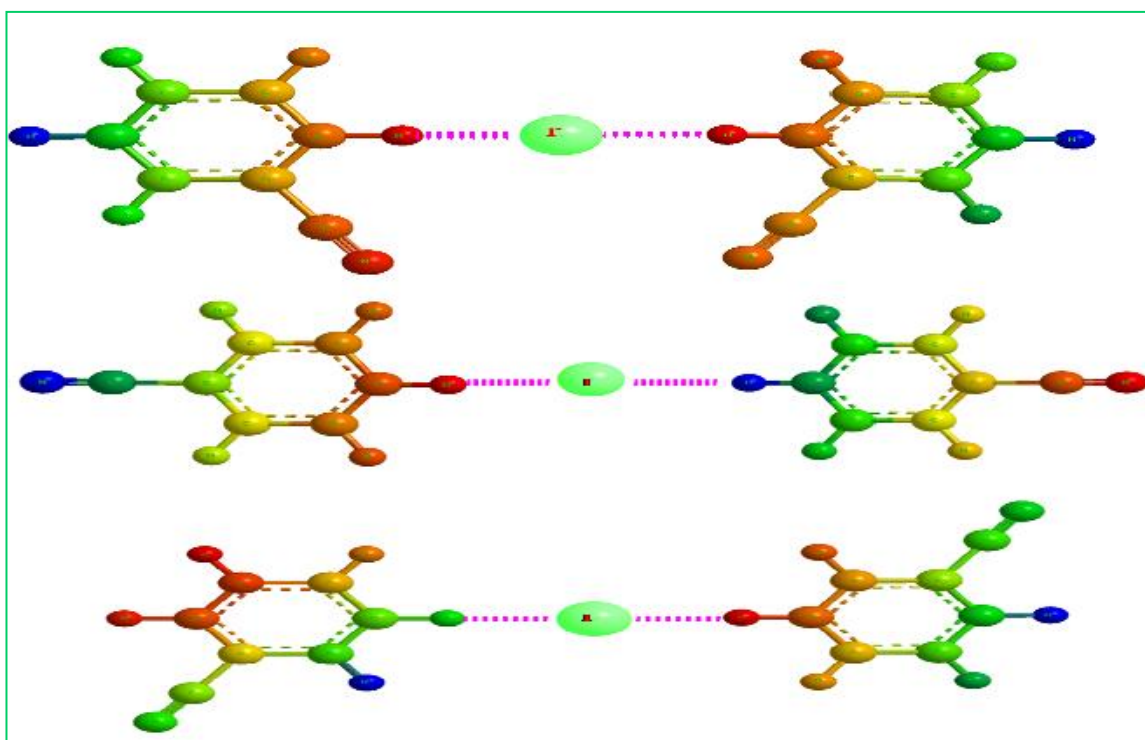
**Figure 10.** Fluorescence emission spectra of Benzonitrile in the presence of 0.1mM– 1.0 mM of Lithium iodide. ( $\lambda_{ex}$  =113nm, slit =5/5)

## Schemes

Scheme 1. Optimised geometry would involve a central  $\text{Li}^+$  ion tetrahedrally surrounded by four benzonitrile molecules



Scheme2. Diagrammatic representation of the Probable Geometrical Configurations of the complex  $I(\text{PhcN})_2^-$



Published in **Chemical Physics Letters** 671 (2017) 7–14

